

Estimation of the discharge current and extracted current from the Penning ion source

© M.S. Lobov,¹ I.M. Mamedov,^{1,2} N.V. Mamedov,^{1,2} A.I. Presniakov,¹ V.I. Zverev,^{1,2} D.I. Iurkov^{1,2}

¹ Dukhov All-Russia Research Institute of Automatics, Moscow, Russia

² National Research Nuclear University „MEPhI“, Moscow, Russia

e-mail: lobovms@yandex.ru

Received February 8, 2023

Revised March 27, 2023

Accepted March 27, 2023

A Penning ion source for a miniature linear accelerator is investigated. A discharge current dependence on the anode voltage for several pressure values is calculated. The estimates are based partly on simplified theoretical models, partly on experimental data obtained on previous work. The ion current component is selected from the obtained dependences and the ion current component value, extracted from the ion source, is estimated. The extracted current dependences and the ion extraction efficiency coefficient value on the voltage at the anode at different source output aperture diameters are calculated.

Keywords: Penning ion source, miniature linear accelerator, discharge current-voltage characteristics, extracted current.

DOI: 10.61011/TP.2023.06.56526.16-23

Introduction

Penning ion sources (PIS), despite a long history of study and improvement, continue to be one of the most popular types of ion sources (IS), used, in particular, in miniature linear accelerators (MLAs) [1,2]. In this regard, the optimization of various PIS parameters is extremely relevant [2–11], despite the long history of study in this area [2]. These parameters include: physical (anode voltage, working gas pressure, magnetic field induction) and geometric (radius and length of the anode, distance between cathodes, cathode diameters, extraction hole diameter, anticathode) shape.

Experimental studies [3–16] describe a large number of compact PIS developed specifically for MLAs, which differ greatly both in their geometric parameters and physical characteristics (anode voltage, magnitude and configuration of the magnetic field etc.). It can also be seen from the presented modern works that the empirical approach to determining the optimal geometric parameters of the discharge cell and power supply parameters prevails. Thus, the papers describe ISs with different sizes and different configurations of the magnetic field, while the parameters of specific experiments differ in details. Therefore, it is extremely difficult to adequately compare experimental data and use the obtained conclusions when creating PIS for MLA.

Besides, there are a number of theoretical papers and numerical models of particles behavior in PIS [17–30]. In models both commercial and developed by researchers the different approaches are used starting from calculations in single-particle approximation [17–22], programs based on the PIC method and MCC (Monte-Carlo calculation) [23–26], and ending with „magnetohydrodynamic“ models that use the first moments the kinetic equation or the balance

equation for the number of particles, pulse and energy [27–30]. Moreover, if before the appearance of powerful computing tools the emphasis was on simplifying formulas with the help of clear physical assumptions [30], then now we are speaking about approaching the ideology of „digital twin“ [11,23,25] of a specific MLA. This brings magnetohydrodynamic approaches closer to „simulation“ approaches, the purpose of which is specifically calculation of all performance data of specific PIS in MLA [11,23,25]. Unfortunately, all these theoretical approaches do not make it possible to quickly and relatively simply obtain practical data, in particular, the CVC of the discharge and the current of the extracted ion beam, for specific MLAs.

Contradictory experimental data and incomplete results of numerical simulations prompt once more to address the classical theoretical papers to establish some general, fundamental regularities in the burning modes of this type of discharge. It is necessary to understand the effect of the physical (especially the magnitude of the magnetic field and the anode voltage) and geometric parameters of the discharge on its burning mode. It would also be valuable to find calculation estimation („engineering“) formulas for a quick assessment of the discharge current, electron density in the discharge, discharge potential, and the ion current extracted from the source. The obtained knowledge would allow the results extrapolation of the specific design study [5,7,8] to the entire class of such devices.

The purpose of this paper is to perform evaluation calculations of CVC of the particular PIS for MLA [7,8] on the basis of relatively simple models and equally simple experiments performed in a continuous mode of supply and with hydrogen as working gas. Estimates of the extracted

current and extraction coefficient, as well as their validation by comparison with experimental data, are necessary for further use in optimizing the operating parameters of MLAs and their power supply diagrams [5].

1. How the Penning ion source works

The simplified diagram of PIS is presented in Fig. 1. Two cathodes with negative potential relative to the anode (usually made in the form of a ring or a cylinder) are placed in a longitudinal (directed parallel to the axis of the system) magnetic field. Most often, cylindrical magnetic rings are used, located behind the PIS body. In the absence of the magnetic field, the primary electrons leaving the cathode move along electric field lines that are perpendicular to the cathode surface and bend towards the anode. These electrons will have both radial and longitudinal velocity components. Axial electrons with minimum radial velocity begin to oscillate between the cathodes, the remaining „radial“ electrons immediately move towards the anode.

When applying the magnetic field parallel to the axis of the system, the trajectories of electrons change and their paths increase [17]. Along z axis the electron performs harmonic oscillations with a frequency the greater, the greater the applied voltage and the shorter the distance between the electrodes are. In the plane $r\Theta$ the electron describes a cycloid or a spiral, while it oscillates around a

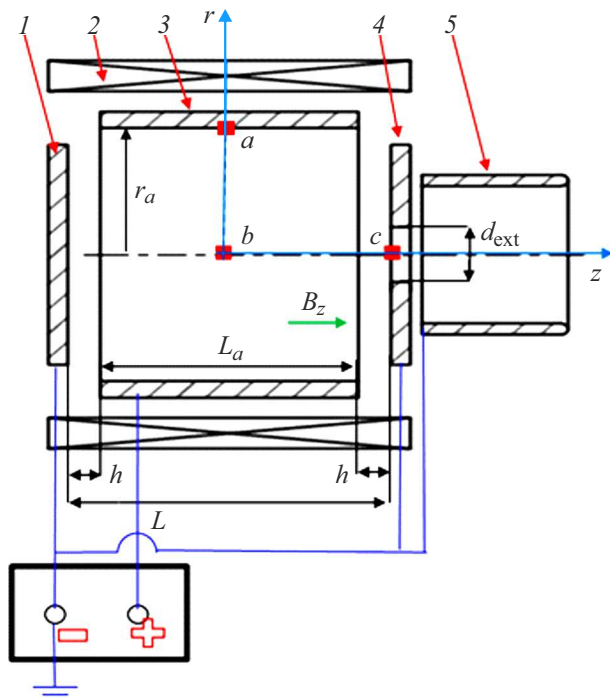


Figure 1. Simplified PIS diagram: 1 — cathode, 2 — magnets, 3 — anode, 4 — anticathode, 5 — focusing electrode (at cathode potential); $r_a = 6$ mm — anode radius, $L_a = 15$ mm — anode length, $L = 20$ mm — cell length, $h = 2.5$ mm — gaps between anode edges and cathodes, $d_{ext} = 8$ mm — PIS outlet aperture diameter.

certain middle position and participates in rotational motion with a frequency slightly less than the Larmor frequency. Thus, there is an elongation of the path passed by electrons in the discharge chamber, which increases the efficiency of the working gas ionization inside the discharge cell. The investigated PIS is used in MLA and is described in [5,7,8].

2. Estimates of the discharge current by known analytical formulas

In several review foreign articles [17,18] and in a number of publications of domestic scientists [19–21] the results of studies of the Penning discharge as applied to pressure gauges and ion pumps are summarized. In particular, the burning modes of this discharge were identified depending on its physical parameters (voltage at the anode, magnetic field strength, and working gas pressure). For different burning modes of discharge the theoretical expressions are obtained for the dependence of the potential of the discharge cell center, the electron density, and the discharge current on the physical parameters and geometrical parameters of the discharge cell (the radius and length of the anode, the distance between the cathodes).

The author of the paper [17], based on the classical formula for the electrons mobility in a transverse magnetic field, obtained expressions relating the value of the potential sag to the discharge current (the formulas are written in SI):

$$U_a - U_0 = \frac{3e}{16m} \frac{\vartheta_i}{\vartheta_c} r_a^2 B^2, \quad (1)$$

$$I_{discharge} = \frac{3e}{4m} \pi l_a \varepsilon_0 \frac{\vartheta_i^2}{\vartheta_c} r_a^2 B^2. \quad (2)$$

Therefore, the discharge current is

$$I_{discharge} = 4\pi l_a \varepsilon_0 \vartheta_i (U_a - U_0), \quad (3)$$

where $\varepsilon_0 = 8.85 \cdot 10^{-12} \text{ C}^2 \cdot \text{m}^{-3} \cdot \text{kg}^{-1} \cdot \text{s}^2$, l_a — anode length, $(U_a - U_0)$ — difference between the anode potential and the potential at the center of the discharge cell, ϑ_i — ionization frequency, ϑ_c — collision frequency of electrons with neutral gas, r_a — anode radius, B — magnetic induction.

This formula was obtained for „infinitely long“ cell, i.e., by neglecting the dependences of all characteristic parameters of the discharge on the axial coordinate (z). In this case, the key parameter is the potential of the center of the Penning cell, which is determined by the presence of a negative bulk charge. It is easy to see that it depends on the magnetic field and implicitly on the anode voltage — due to the ionization frequency dependence on the electron velocity, which depends on the anode potential.

Based on formula (3), we can obtain the following evaluation expressions for the discharge current (working gas—hydrogen):

$$I_{discharge}[A] = 7.7 \cdot 10^{-2} l_a[m] p[\text{Torr}] (U_a - U_0)[V]. \quad (4)$$

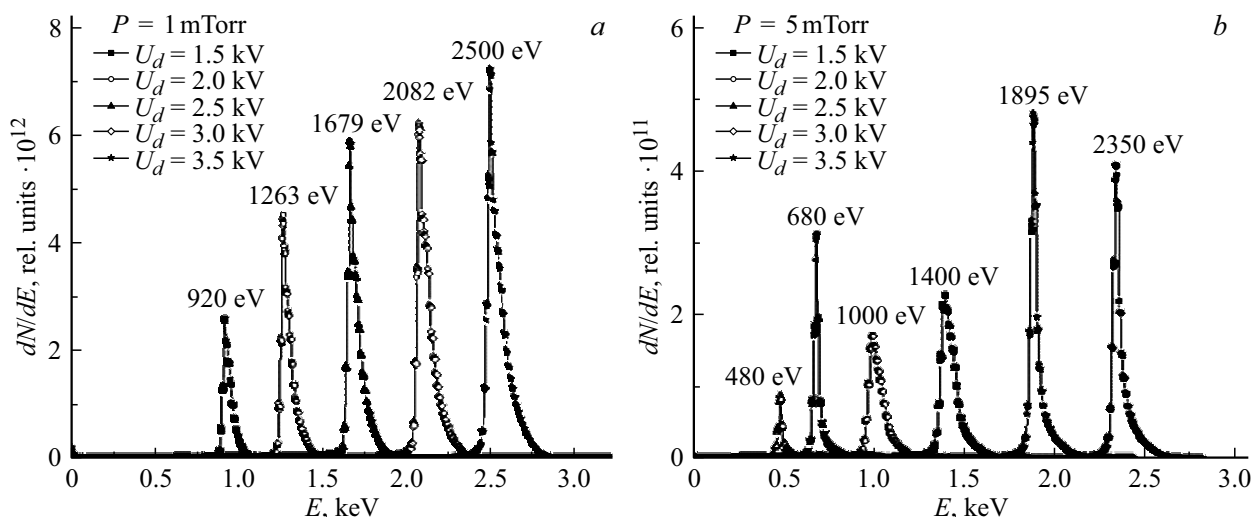


Figure 2. Families of energy spectra of extracted ions at different voltages across the discharge gap: *a* — 1, *b* — 5 mTorr [31,32]. The numbers designate the maxima in the energy spectra.

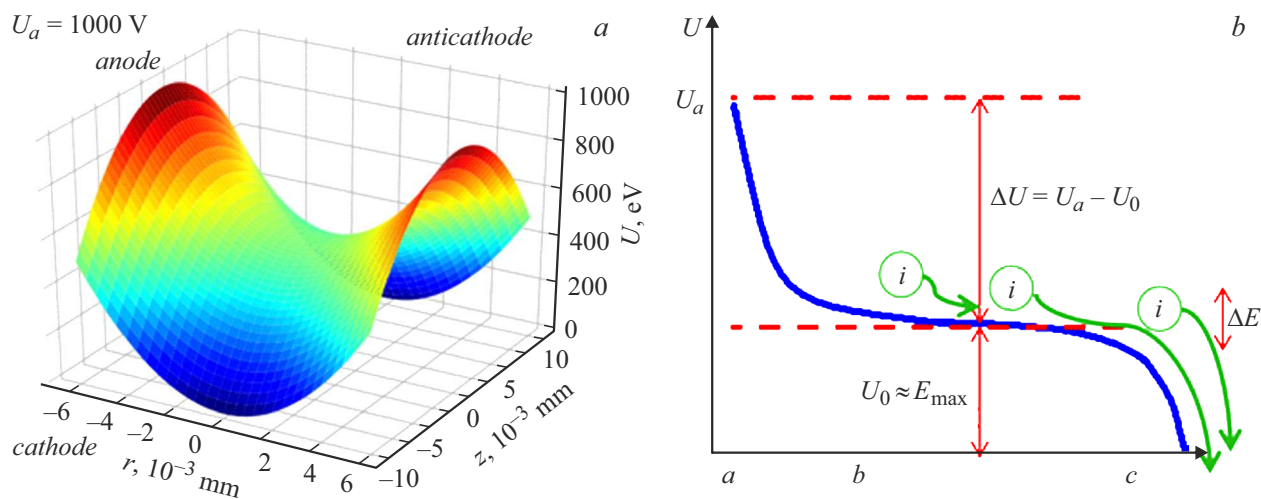


Figure 3. *a* — 3D-potential distribution inside the discharge cell (anode voltage 1 kV), *b* — characteristic potential distribution curve inside the discharge cell for the anticathode with a hole (along radius *ab*, along axis *bc*) when measuring the energy spectra of extracted ions. Dots *a, b, c* (see Fig. 1) designate: *a* — anode, *b* — cell center, *c* — anti-cathode.

For the source under study, the anode length $l_a = 15$ mm, the anode radius $r_a = 6$ mm, and the magnetic induction value $B = 80$ mT. The ionization frequency was „upper“ estimated by the formula: $\nu_i = n_0 v_i \sigma_i$, where $v_i = 2.35 \cdot 10^6$ m/s — electron velocity for ionization, $\sigma_i \approx 10^{-20}$ m² — maximum ionization cross section for hydrogen molecules, $n_0[\text{m}^{-3}] = 3.5 \cdot 10^{22}$ p [Torr] — concentration of neutral particles as a function of pressure. To determine the center potential U_0 of the cell in the burning discharge, we measured the energy spectra of the extracted (in the longitudinal direction) ions at various anode voltages and pressures [31,32]. The general form of the obtained energy spectra (see, for example, [31,32] and Fig. 2) can be qualitatively interpreted as follows. In the central part of the discharge, with the exception of the near-cathode regions,

the potential is almost constant along the axis. Therefore, the vast majority of ions formed in this region, passing through the same difference in the near-cathode potential drop, acquire approximately the same energy at the PIS exit (Fig. 3). Thus, it can be assumed that the maximum of the energy spectrum (of emitted ions) is equal to the potential at the center of the discharge cell $E_{\text{max}}/e \sim U_0$ (Fig. 2, 3).

Due to the potential sag on the source axis, the energy spectrum of the emitted ions is shifted to the low-energy region. The sharp increase in the energy spectrum (left part of the spectrum) can be explained by the fact that some of the ions formed within the plasma boundary layer near the anti-cathode (in the region of the cathode potential drop) acquire energy different from the ions produced in the plasma volume. „The high-energy tail“ in

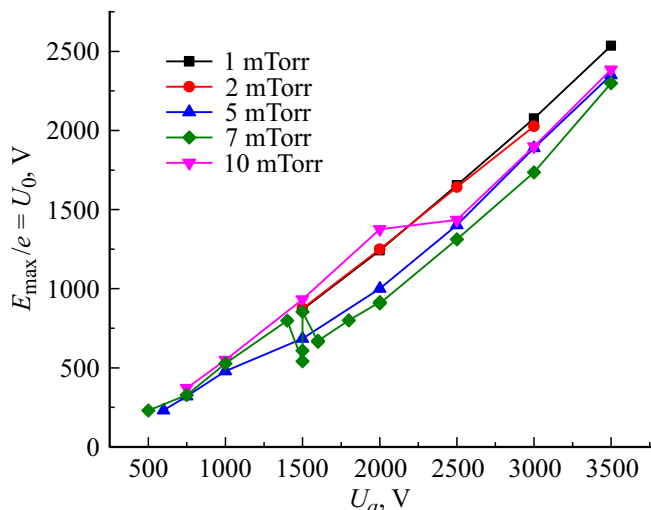


Figure 4. Energy spectrum maximum vs. anode voltage at various pressures. based on data from papers [31,32].

the energy spectrum (right part of the spectrum) is due to the registration of the ions from the plasma volume (i.e., at a some distance from the axis), where the value of the plasma potential is noticeably greater than the potential on the axis [33]. Fig. 4 shows the dependence of the energy spectrum maximum on the anode voltage at various pressures. The energy spectra were registered using a quarter-spherical electrostatic deflector with energy resolution of 0.8 to 1.5% [31,32]; therefore, the error in determining the maximum of the energy spectrum is maximum 2%. Thus, the magnitude of the potential sag is defined as the difference between the applied voltage at the anode and the maximum in the resulting energy spectrum $\Delta U = U_a - E_{max}/e$. Therefore, having determined the value of U_0 , it is possible to calculate CVC of the discharge at various pressures of the working gas using formula (4).

3. Estimation of the discharge current taking into account the ionization frequency dependence on energy

As can be seen from formula (3), the dimension of $\varepsilon_0 U$ corresponds to the linear charge density [C/m], therefore, when multiplied by the anode length [m] and ionization frequency [1/s] we obtained the dimension of current [A]. Therefore, it is tempting to use this simple expression to estimate the discharge current in ion sources for MLA. The only question is how to express the ionization frequency more accurately, i.e., take into account the change in the kinetic energy of the electron when moving inside the Penning cell, since when deriving formulas (3) and (4) it was stipulated that the ionization frequency is constant. Thus, it is necessary to replace the functional dependence of the ionization frequency on energy (which depends on the potential difference of the electric field) with dependences

on coordinates in the cell volume, and then, by integration average the expression for the discharge current within the geometric limits of this cell. This assumption is appropriate, since, according to [22,34] the main contribution to the ionization process is made by electrons oscillating along the cell axis, so that their velocity and, accordingly, the kinetic energy, which determines the ionization cross-section and frequency, are rapidly oscillating functions of time and coordinates. According to [35], electrons oscillating along the axis z create only „primary secondary“ electrons, which further develop an avalanche along the radius r . Then the ionization frequency as a function of local coordinates has the form:

$$\begin{aligned} \vartheta_i &= n_0 v_i(E_{kin}) \sigma_i(E_{kin}) \rightarrow \vartheta_i = n_0 v_i(U(z, r)) \sigma_i(U(z, r)) \\ &\rightarrow \vartheta_i = n_0 v(z, r) \sigma_i(z, r). \end{aligned} \quad (5)$$

Then the speed and kinetic energy of the electron as a function of local coordinates are determined from the energy conservation law under the assumption that the initial energy of the electron is zero (more precisely, its value is small compared to the characteristic voltage at the anode — about 1 kV):

$$v(r, z, U_a) = \sqrt{\frac{2e}{m_e} U(r, z, U_a)}, \quad (6)$$

where e and m_e — absolute values of the electron charge and mass, U_a — voltage at the anode, $U(r, z, U_a)$ — potential at point (r, z) of the cell.

The potential distribution in the real Penning cell, even in the absence of free space charge in its volume, is inhomogeneous, and the potential at the center differs from the anode potential. For the idealized cell not perturbed by the presence of charges (Fig. 1), the potential distribution can be estimated in three ways. The first option is the calculation of the field distribution taking into account geometric features using commercial codes (for example, Comsol Multiphysics (Fig. 3, a), CST Studio Suite).

The second way is to calculate the potential at each cell point using the quadratic formula [20]:

$$U(r, z) = U_0 \left(1 + \frac{U_a - U_0}{U_0} \frac{r^2}{r_a^2} - \frac{z^2}{L^2} \right), \quad (7a)$$

where r_a — anode radius, L — cell length, U_0 — cell center potential ($z = 0, r = 0$), U_a — anode potential.

And the third option: the potential distribution can be estimated by solving the Dirichlet problem for the Poisson equation [36]. The additional condition for the adequacy of such an estimate is the assumption that the IS operation occurs in „mode of probe measurements“ [37], so that the field extracting ions (from the PIS output aperture) does not significantly change the fields distribution in IS cell. The desired distribution can be represented as a sum of potentials: with homogeneous zero conditions on the cathodes and inhomogeneous on the lateral surface, as well

as with homogeneous condition on the lateral surface and inhomogeneous on the anti-cathode (on the cathode the boundary condition is assumed to be homogeneous):

$$\phi(r, z) = \varphi(r, z) + \varphi_1(r, z), \quad (7b)$$

where

$$\varphi(r, z) = \frac{2}{L} \sum_{k=1}^{\infty} a_k \frac{I_0(k\pi r/L)}{I_0(k\pi r_a/L)} \sin(k\pi z/L),$$

$$a_k = \int_0^L \phi(r = r_a, z) \sin(k\pi z/L) dz,$$

$$\varphi_1(r, z) = \sum_{k=1}^{\infty} b_k \frac{\text{Sh}(\mu_k^{(0)} z/r_a)}{\text{Sh}(\mu_k^{(0)} L/r_a)} J_0\left(\frac{\mu_k^{(0)} r}{r_a}\right),$$

$$b_k = \frac{2}{r_a^2 J_1^2(\mu_k^{(0)})} \int_0^{r_a} F(r) J_0\left(\frac{\mu_k^{(0)} r}{r_a}\right) r dr,$$

r_a, L — cell radius and length, $\phi(r = r_a, z)$ — potential on the side generatrix, J_k — corresponding Bessel functions, I_k — corresponding modified Bessel functions, $\mu_k^{(0)}$ — function zeros J_0 , $F(r)$ — potential distribution over the anti-cathode surface, from the hole in which extraction is performed. The unknown functions in this solution are the potential distributions on the side surface in the gaps between the cathodes and the anode, as well as the potential distribution in the anti-cathode plane within the hole. If the first functions, due to the small size of the gaps in the studied PIS, can be taken linear with a sufficient degree of accuracy, then the latter function shall be calculated using some additional conditions. The „potential sag“ in PIS output aperture can be considered in a parabolic approximation, the parameters of which can also be taken from the simulations in Comsol Multiphysics package.

The ionization cross-section is calculated using the Thomson formula for molecular hydrogen with ionization potential $I'_i = 15.5$ eV. We will assume that the plasma is formed in PIS, mainly consisting of molecular hydrogen ions [31]:

$$\sigma_i(r, z, U_a) = \sigma_0 \left(\frac{I_i}{U(r, z, U_a)} \right)^2 \frac{U(r, z, U_a) - I'_i}{I'_i}, \quad (8)$$

where $\sigma_0 = 4\pi r_0^2$, IFx61x E m — Bohr radius, IFx62x E eV .

Thus, due to the ionization frequency and the axis potential dependence on the axial coordinate, „the upper estimate“ of the discharge current can be obtained as an integral over the axial coordinate of the product of the ionization frequency and the potential difference between the anode and the cell center, taken within the anode height. The dependence of the frequency and potential on the radial coordinate can be taken into account by averaging, i.e., by integrating over the radius. To obtain more accurate dependences, it is necessary to take into account the fact

that only those electrons whose cyclotron radius is not less than their distance from the anode at a given point can get to the anode. In other words, the lower integration limit in the formula for the current shall be taken as the difference between the anode (cell) radius and the Larmor radius. It is clear that if it is equal to zero, the limits coincide and the integral is also equal to zero. On the contrary, the difference of limits takes the maximum value at the point where the cyclotron radius is maximum. Thus, the entire integral over the radial coordinate becomes the function z :

$$I_{\text{discharge}}(U_a) = \frac{4\pi\epsilon_0}{r_a} \int_h^{L-h} \int_{r_a-R_B}^{r_a} \vartheta_i(r, z, U_a) \times (U_a - U(r, z, U_a)) dr dz, \quad (9)$$

where the Larmor (cyclotron) radius is determined for a constant axial magnetic field B according to the well-known formula:

$$R_B(r, z, U_a, B) = \frac{m_e}{e} \frac{v(r, z, U_a)}{B}. \quad (10)$$

The reasoning described above is acceptable, since for the characteristic parameters of the Penning cell — $L \sim 2$ cm, $R \sim 1$ cm, $U_a \sim 1$ kV, $B \sim 50$ mT, $P_{\text{H}_2} \sim 1$ mTorr — we obtain the following characteristic frequencies: cyclotron $\Omega = 8.8$ GHz, oscillation frequency $\omega_{\text{osc}} \approx 1.6$ GHz, the transport frequency is 4.8 MHz, and the ionization frequency is by an order of magnitude lower. With such Larmor parameters, the (cyclotron) radius is less than 0.25 mm. Thus, taking into account collisions has practically no effect on the nature of the motion, due to the very large difference in frequencies — the electron has time to complete about 300 oscillations before experiencing the elastic collision, leading to insignificant loss of kinetic energy, but (possibly) significant change in pulse. The trajectory is actually a straight line „stretched“ on the magnetic field line, since the Larmor (cyclotron) radius is less than 0.25 mm. Therefore, for „cathodic“ electron almost all kinetic energy is the energy of axial motion. Accordingly, the electron energy distribution function (EDF) is strongly anisotropic, so that the main part of electrons with high kinetic energy does not participate in the charge transfer process [38], but in the ionization process only. It is clear that the approach based on solving the kinetic equation with various known forms of the isotropic part is inapplicable in this case. It is clear that for electrons starting from „anti-cathode“ the picture will be the same. Only for electrons starting from the very periphery of the cathodes, where the radial component of the electric field is large, the contribution of the radial and azimuthal motions will increase somewhat. In the same way, this contribution will also increase for plasma electrons produced in the cell volume as it approaches its middle.

Formula (9) also takes into account additional geometrical parameters of PIS: cell length $L = 20$ mm, gaps between

the anode edges and cathodes $h = 2.5$ mm. As can be seen, as the magnetic induction tends to zero, the Larmor radius tends to infinity, and the lower limit may turn out to be negative, which will lead to an imaginary increase in the calculated current. Therefore, if the Larmor radius coincides with or exceeds the cell radius, the integral is assumed to be equal to zero. Accounting for the secondary ion-electron emission coefficient γ , according to [18], will lead to the multiplication of formulas (9) by $(1 + \gamma)$. Usually [17] γ is taken in the range of 0.03–0.05 regardless of the anode voltage (which affects the energy with which the ion hits the cathode). In the paper [34] a semi-empirical formula for determining the coefficient of secondary electron emission is proposed: $\gamma = 0.0253\sqrt{U_a}$.

4. Estimate of extracted ion current

This ideology of current calculation through the voltage in the cell volume and the ionization frequency can also be used to estimate the ion current to the cathodes. Moreover, unlike „magnetized“ electrons all ions produced in the „cathode“ half of the cell fall on the cathode, while the anti-cathode is achieved by ions born in the „anti-cathode half“ only, which are not extracted through the output aperture of the cell. So, the ionic component of the discharge current shall also be written as the sum of two double integrals (over r and z — integration over the angle is replaced by multiplication by 2π due to axial symmetry) with different limits of integration:

$$I_{ion} = \frac{4\epsilon_0}{Lr_a} \int_0^{L/2} \int_0^{r_a} \vartheta_i(r, z, U_a)U(r, z, U_a)rdrdz + \frac{4\epsilon_0}{L(r_a - \frac{d_{ext}}{2})} \int_{L/2}^L \int_{d_{ext}/2}^{r_a} \vartheta_i(r, z, U_a)U(r, z, U_a)rdrdz, \quad (11)$$

where $d_{ext} = 8$ mm — diameter of PIS output aperture (holes in „anti-cathode“). In (11) the following is taken into account:

- cathode potentials are equal to zero, so the integrals contain simply the value of the potential, but not the difference;
- there is no need to consider the secondary ion-electron emission in this case;
- when averaging over the axial coordinate, division by $0.5L$ is performed, so the numerator still contains 4, and not 2;
- the numerator does not contain π due to averaging over the cathode area.

Based on similar considerations, the output ion current can also be calculated in the form of the corresponding

integral:

$$I_{ext} = \frac{8\epsilon_0}{Ld_{ext}} \int_{L/2}^L \int_0^{d_{ext}/2} \vartheta_i(r, z, U_a)U(r, z, U_a)rdrdz. \quad (12)$$

5. Estimation results

In accordance with formulas (9), (11), (12), the electron (to anode) and ion (to cathodes) discharge currents and the ion current extracted from the source were calculated for five working gas pressures: 1, 2, 5, 7, 10 mTorr. In calculations, the double integral is represented through two integrals, each of which was calculated from a function of one variable. Numerical integration was carried out using the trapezoidal method (in Python Anaconda software package). To reduce the calculation time, the integration grid step was taken equal to 1000 (a further increase in this value did not lead to serious changes in the results). The values of the cell center potential were taken on the basis of the experimental data obtained from the energy spectra [31,32].

The calculation results are shown in Fig. 5, and they also show the experimental results [31]. Note that in the paper [31] the current extracted from the source was measured by a plate located at a distance of 5 mm from the focusing electrode of IS, while the ion beam was not additionally accelerated.

As can be seen from Fig. 5, the measured CVCs are in good agreement with the theoretical dependences. It can be seen from these graphs that at pressures above 5 mTorr (working gas — hydrogen) the sharp jumps in CVC occur, after which a — smooth slow increase in the discharge current with voltage increasing at the anode; at pressures below 5 mTorr the linear increase in the discharge current is seen with the increase in the anode voltage. Papers [17–20] inform that at certain combination of magnetic field, pressure and anode voltage at the moment of transition to another burning mode of discharge the potential decreases in the cathode region, which leads to the change in the potential in the center of the discharge cell and, as a result, to jumps in the discharge current and the extracted current.

These interpretations qualitatively agree with the experiments [39], which it showed that current jumps correspond to changes in the nature, shape, and region of the discharge burning. As can be seen from the obtained results, the total dependence of the discharge current, calculated by expression (12), is less than the experimental curve by 30–50%, except for the case at pressure $P = 1$ mTorr. Such a large error can be attributed both to the incorrect averaging procedure and to the correctness of the chosen approach to the ionization frequency consideration. Nevertheless, the external form of the calculated dependence repeats the form of the experimental one. Thus, even a 50% mismatching

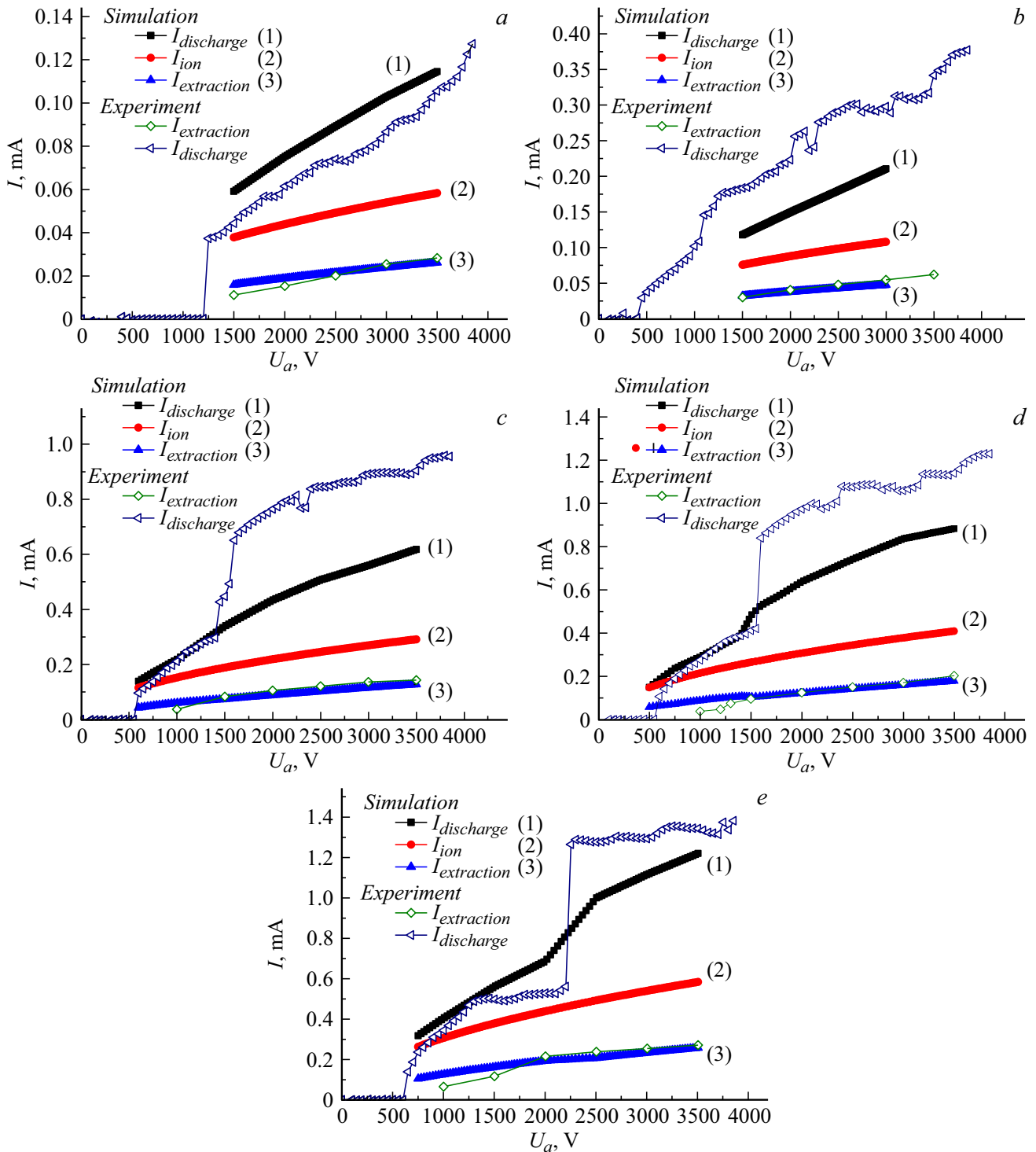


Figure 5. Electron (I) and ion (2) discharge currents and ion current (3) extracted from the source, calculated by expressions (11), (13), (14), respectively depending on the anode voltage (for working gas pressures $P = 1, 2, 5, 7, 10$ mTorr).

with the experiment can be considered acceptable, based on the validity of the estimate, and also taking into account the purpose of the calculation — identifying the main trends, and not finding the exact matching.

In this case, the calculated value of the extracted current is in good agreement with the experimental data, as can be

seen from the graphs presented, — the relative deviation from the experimental values in most cases is only 4–5%.

Also note that the obtained estimation formulas (in contrast to the paper [40]) do not require the calculation of the ion mobility coefficient and the width of the region of the dark cathode space.

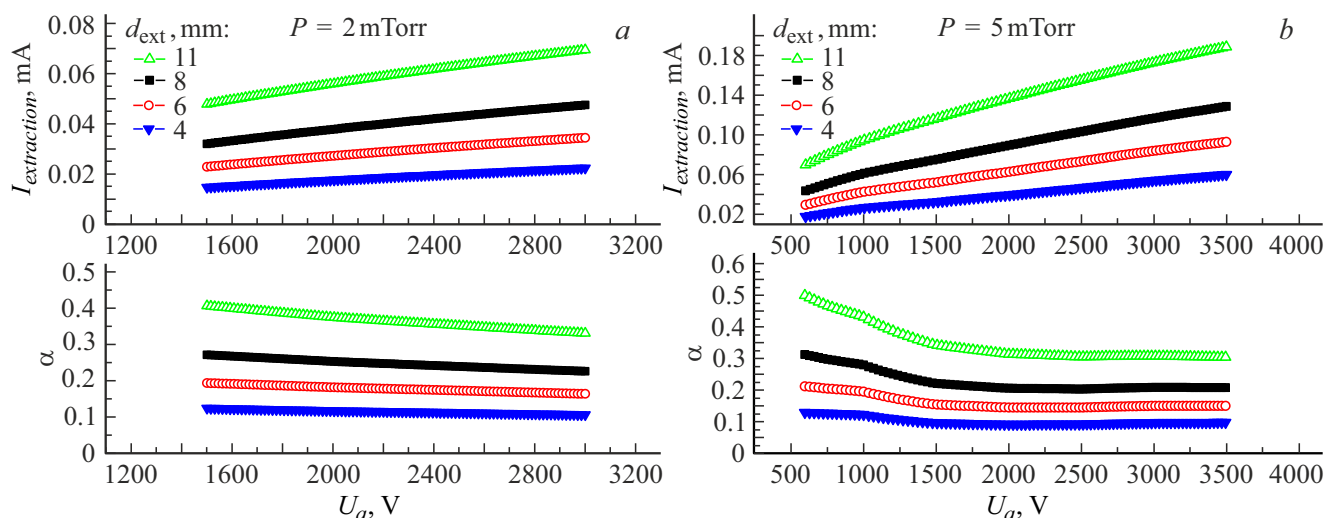


Figure 6. Calculated extracted current and calculated values of the ion extraction efficiency coefficient IFx77x E vs. anode voltage at different output aperture diameters ($P = 2$ and 5 mTorr).

6. Change of the extracted current during varying the output aperture

Based on the considerations given above, it is possible to vary the diameter of the output aperture, assuming, of course, that the discharge burning mode and, as a consequence, the potential distribution inside the cell do not change in this case. Based on general considerations, it is obvious that the maximum of the extracted current will be reached when $d_{\text{ext}}/2 \rightarrow r_a$, i.e., the maximum extracted current is equal to half of the ion current in the cell in the absence of a diaphragm. It is interesting to answer how the ion extraction efficiency factor will change in this case ($\alpha = I_{\text{extraction}}/I_{\text{discharge}}$). Fig. 6 shows the calculated extracted current and the calculated values of the ion extraction efficiency factor vs. the anode voltage for various output aperture diameters ($P = 2$ and 5 mTorr). This pressure was chosen as the most probable working pressure inside the MLA, determined in the papers [7,8].

From the graphs presented, one can see the quite expected result — with increase in the diameter of the output aperture, the value of the extracted current and the ion extraction efficiency coefficient α increase. With the increase in the diameter from 4 to 11 mm, the ion extraction efficiency coefficient IFx77x E increased from 0.1 to 0.4 for all studied anode voltages and pressures. A further increase in diameter does not lead to a noticeable increase in the extraction factor.

Conclusion

The possibility of theoretical calculation of the potential of the discharge cell center and the electron concentration using expressions for the average ionization probability is shown.

For the existing IS design used in the MLA, the dependence of the voltage discharge current on the anode was calculated for several pressure values. From the dependences obtained the ion current to PIS cathodes was identified, and the value of the ion current extracted from the cell was estimated. The calculated discharge current is in satisfactory agreement with the experimental values (the mismatching with the experiment is maximum 50%). The possibility of using analytical calculations to obtain the general view of the dependences of the main characteristics of PIS and the main trends in changes in characteristics with a slight variation in the PIS geometry is demonstrated. In this case, the relative deviation of the calculated value of the extracted current from the experimental values in most cases is only 4–5%.

The dependence of the extracted current and the value of the ion extraction efficiency coefficient on the anode voltage for various output aperture diameters are calculated. It is shown that with increase in the diameter from 4 to 11 mm, the ion extraction efficiency coefficient α increased from 0.1 to 0.4 for all studied anode voltage and pressures.

Acknowledgments

The authors are grateful to N.N. Shchitov, Ph.D. for valuable comments and constructive suggestions for improving the text of the article.

Conflict of interest

The authors declare that they have no conflict of interest.

References

- [1] V. Valkovic. *14 MeV Neutrons. Physics and Applications* (CRC Press Taylor & Francis Group, Boca Raton, London, NY., 2016)
- [2] F.M. Penning, J.H.A. Moubis. *Physica*, **IV** (11), 71 (1937).
- [3] X. Zhou, J. Lu, Y. Liu, X. Ouyang. *Nucl. Inst. Methods Phys. Res. A*, **987**, 164836 (2021). DOI: 10.1016/j.nima.2020.164836
- [4] X. Zhou, Y. En, J. Lu, Y. Liu, K. Li, Zh. Lei, Zh. Wang, X. Ouyang. *Instrum. Experiment. Techniq.*, **63**(4), 595 (2020). DOI: 10.1134/S002044122004020X
- [5] R.S. Rachkov, A.Y. Presnyakov, D.I. Yurkov. *At. Energ.*, **126** (6), 383 (2019). DOI: 10.1007/s10512-019-00569-3
- [6] A. Zhang, D. Li, L. Xu, Z. Xiong, J. Zhang, H. Pengand, Q. Luo. *Phys. Rev. Accelerators and Beams*, **25** (10), 103501 (2022). DOI: 10.1103/PhysRevAccelBeams.25.103501
- [7] N.V. Mamedov, S.P. Maslennikov, A.A. Solodovnikov, D.I. Yurkov. *Fizika plazmy*, **46** (2), 172 (2020) (in Russian).
- [8] N.V. Mamedov, S.P. Maslennikov, Yu.K. Presnyakov, A.A. Solodovnikov, D.I. Yurkov. *Tech. Phys.*, **64** (9), 1290 (2019). DOI: 10.1134/S1063784219090081
- [9] W. Liu, M. Li, K. Gao, D. Gu. *Nucl. Instrum. Methods Phys. Res. A*, **768**, 120 (2014). DOI: 10.1016/j.nima.2014.09.052
- [10] A. Fathi, S.A.H. Feghhi, S.M. Sadati, E. Ebrahimibasabi. *Nucl. Instrum. Methods Phys. Res. A*, **850**, 1 (2017). DOI: 10.1016/j.nima.2017.01.028
- [11] M. Xie, D. Liu, L. Liu, H. Wang. *AIP Advances*, **11**, 075123 (2021). DOI: 10.1063/5.0057038
- [12] M. Li, W. Xiang, K.X. Xiao, L. Chen. *Rev. Sci. Instrum.*, **83**, 02B722 (2012). DOI: 10.1063/1.3675386
- [13] N.V. Mamedov, A.V. Gubarev, V.I. Zverev, S.P. Maslennikov, A.A. Solodovnikov, A.A. Uzvolok, D.I. Yurkov. *Plasma Sources Sci. Technol.*, **29**, 025001 (2020). DOI: 10.1088/1361-6595/ab6758
- [14] A.N. Dolgov, V.G. Markov, I.A. Kanshin, D.E. Prokhorovich, A.G. Sadilkina, I.V. Vizgalov, V.I. Rashchikov, N.V. Mamedov, D.V. Kolodko. *J. Phys.: Conf. Series*, **666**, 012023 (2016). DOI: 10.1088/1742-6596/666/1/012023
- [15] D. Xin, C. Zhao, Q. Xu, S. Qiao. *Nucl. Inst. Methods Phys. Res. A*, **903**, 147 (2018). DOI: doi.org/10.1016/j.nima.2018.05.060
- [16] F.W. Abdel Salam, H. El-Khabeary, M.M. Ahmed, A.M. Abdel Reheem. *Rev. Sci. Instrum.*, **82**, 033304 (2011). DOI: 10.1063/1.3554637
- [17] W. Schuurman. *Physica*, **36**, 136 (1967).
- [18] E.B. Hooper Jr. *A review of reflex and Penning discharges, in Advances in Electronics and Electron Physics* (Academic Press, NY., 1969), v. 27.
- [19] E.M. Reichrudel, G.V. Smirnitckaya, Nguyen Huu Ti. *ZhTF*, **XXXIX** (6), 1052 (1969). (in Russian)
- [20] G.V. Smirnitckaya, Nguyen Huu Ti. *ZhTF*, **XXXIX** (6), 1044 (1969). (in Russian)
- [21] E.M. Reichrudel, G.V. Smirnitckaya, R.P. Babertsyan. *ZhTF*, **XXXVI** (7), 1226 (1966). (in Russian)
- [22] N.N. Schitov, D.I. Yurkov. *J. Phys.: Conf. Series*, **830**, 012056 (2017). DOI: 10.1088/1742-6596/830/1/012056
- [23] Zi-TongYu, Shi-WeiJing, Wen-Juan Zhang, Si-Jia Zhao, Yong Guo. *Optik*, **181**, 914 (2019). DOI: 10.1016/j.ijleo.2018.12.166
- [24] Z. Yu, S. Zhao, W. Guo, Y. Zheng, S. Jing, W. Zhang. *Optik*, **213**, 164789 (2020). DOI: 10.1016/j.ijleo.2020.164789
- [25] N.V. Mamedov, A.S. Rohmanenkov, V.I. Zverev, S.P. Maslennikov, A.A. Solodovnikov, A.A. Uzvolok, D.I. Yurkov. *Rev. Sci. Instrum.*, **90**, 123310 (2019). DOI: 10.1063/1.5127921
- [26] A.S. Rokhmanenkov, S.E. Kuratov. *J. Phys.: Conf. Ser.*, **1250**, 012036 (2019). DOI: 10.1088/1742-6596/1250/1/012036
- [27] S.T. Surzhikov. *ZhTF*, **87** (8), 1165 (2017). (in Russian) DOI: 10.21883/JTF.2017.08.44722.2031
- [28] A.S. Dikalyuk, S.E. Kuratov, M.G. Lobok, D.A. Storozhev. *J. Phys.: Conf. Ser.*, **1250**, 012033 (2019). DOI: 10.1088/1742-6596/1250/1/012033; Sh. Ju, J. Li, J. Lu, X. Zhou. *J. Phys.: Conf. Ser.*, **1601**, 062034 (2020). DOI: 10.1088/1742-6596/1601/6/062034
- [29] S.P. Nikulin. *Rus. Phys. J.*, **44** (9), 969 (2001).
- [30] L.S. Brown, G. Gabrielse. *Rev. Modern Phys.*, **58** (1), 233 (1986).
- [31] N.V. Mamedov, N.N. Shchitov, D.V. Kolodko, I.A. Sorokin, D.N. Sineľnikov. *Tech. Phys.*, **63** (8), 1129 (2018). DOI: 10.1134/S1063784218080121
- [32] N. Mamedov, D. Kolodko, I. Sorokin, I. Kanshin, D. Sineľnikov. *J. Phys.: Conf. Ser.*, **830**, 012063 (2017). DOI: 10.1088/1742-6596/755/1/011001
- [33] P. Rohwer, H. Baumann, K. Bethge, W. Schutze. *Nucl. Instrum. Methods*, **204**, 245 (1982).
- [34] F.K. Chen, *J. Appl. Phys.*, **56**, 3191 (1984). DOI: 10.1063/1.333882
- [35] G.V. Smirnitckaya, Nguyen Huu Ti. *ZhTF*, **XXXIX** (4), 694 (1969). (in Russian)
- [36] B.M. Budak, A.A. Samarsky, A.N. Tikhonov. *Sbornik zadach po matematicheskoy fizike* (Nauka, M., 1972). (in Russian)
- [37] A.V. Gruzdev, V.G. Zaleskii. *Prikladnaya fizika*, **5**, 82 (2009) (in Russian).
- [38] L.A. Zyulkova, A.V. Kozyrev, D.I. Proskurovskii. *ZhTF*, **75** (11), 59 (2005). (in Russian)
- [39] N.N. Shchitov, I.A. Kanshin, N.V. Mamedov. *Fiziko-khimicheskaya kinetika v gazovoy dinamike*, **16** (4), 2 (2015). (in Russian)
- [40] V.T. Barchenko, E.A. Petrova, V.G. Zaleskii. *Vestnik Polotskogo gos. un-ta. Seriya S. Fundamentalnye nauki. Fizika*, **12**, 57 (2012) (in Russian).

Translated by I.Mazurov